



Strongly driven quantum pendulum of the carbonyl sulfide molecule

Sebastian Trippel,¹ Terry Mullins,¹ Nele L. M. Müller,¹ Jens S. Kienitz,^{1,2} Juan J. Omiste,³ Henrik Stapelfeldt,^{4,5}
Rosario González-Férez,^{2,3} and Jochen Küpper^{1,2,6,*}

¹Center for Free-Electron Laser Science, DESY, Notkestrasse 85, 22607 Hamburg, Germany

²The Hamburg Center for Ultrafast Imaging, University of Hamburg, Luruper Chaussee 149, 22761 Hamburg, Germany

³Instituto Carlos I de Física Teórica y Computacional and Departamento de Física Atómica, Molecular y Nuclear, Universidad de Granada, 18071 Granada, Spain

⁴Department of Chemistry, Aarhus University, 8000 Aarhus C, Denmark

⁵Interdisciplinary Nanoscience Center (iNANO), Aarhus University, 8000 Aarhus C, Denmark

⁶Department of Physics, University of Hamburg, Luruper Chaussee 149, 22761 Hamburg, Germany

(Received 27 January 2014; published 5 May 2014)

We demonstrate and analyze a strongly driven quantum pendulum in the angular motion of state-selected and laser-aligned carbonyl sulfide molecules. Raman couplings during the rising edge of a 50-ps laser pulse create a wave packet of pendular states, which propagates in the confining potential formed by the polarizability interaction between the molecule and the laser field. This wave-packet dynamics manifests itself as pronounced oscillations in the degree of alignment with a laser-intensity-dependent period.

DOI: [10.1103/PhysRevA.89.051401](https://doi.org/10.1103/PhysRevA.89.051401)

PACS number(s): 33.80.-b, 37.10.Vz, 37.20.+j

Pendular states, directional superpositions of field-free rotational states, are created by the anisotropic interaction between an isolated molecule and a strong electric field [1–4]. In a classical sense, this corresponds to the free rotation of the molecule changing into a restricted angular motion, where a molecular axis librates about the field direction. In the case of a strong static electric field the pendular states result from the interaction with the permanent dipole moment. This was exploited, for instance, for the simplification of spectroscopic signatures of large molecular clusters [5]. In the case of a nonresonant laser field the pendular states are formed due to the interaction with the molecular polarizability. This interaction constitutes the basis for laser-induced alignment [3,4], the confinement of molecular axes to laboratory-fixed axes defined by the polarization of the alignment field. Notably, in the limit where the laser field is turned on slowly compared to the inherent rotational period(s) of the molecule, the initial field-free rotational states are converted into the corresponding pendular states. This process is called adiabatic alignment [4] and it has found widespread use in molecular sciences [6–11]. The pendular states persist for as long as the laser field is turned on and the molecules return to their initial field-free rotational states upon turning off the laser field, provided this occurs slowly compared to the rotational period(s), τ_{rot} .

Pendular states were investigated through frequency-resolved spectroscopy [12,13] and by photodissociation or Coulomb explosion imaging [4,14]. The former approach probes the field-induced changes of the rotational energy levels, thus the pendular state energies, while the latter approach probes the way the molecules are confined in space, i. e., the orientational character of the pendular states. So far these studies were all performed in the adiabatic limit where the classical signature of the pendular states, i. e., the librational motion of a molecular axis about the field direction, cannot be observed directly. To observe this motion it would

be necessary to create a coherent superposition of pendular states.

Here, we demonstrate that such pendular motion can be induced through the use of a laser pulse with a duration $\tau_{\text{laser}} \sim \tau_{\text{rot}}$ in between the common limits of adiabatic ($\tau_{\text{laser}} \gg \tau_{\text{rot}}$) and impulsive ($\tau_{\text{laser}} \ll \tau_{\text{rot}}$) alignment. The intermediate regime has hitherto only been explored theoretically [15–17]. We performed a combined experimental and theoretical study in this intermediate pulse-duration regime on aligned carbonyl sulfide (OCS) molecules in their absolute ground state. A wave packet of pendular states was created by the rising edge of a 50-ps laser pulse and its propagation was studied during and after the laser pulse.

A schematic of the experimental setup is shown in Fig. 1. In short, a pulsed molecular beam was provided by expanding 500 ppm of OCS seeded in 6 bar of neon through a cantilever piezo valve [18] at a repetition rate of 250 Hz. After passing two skimmers the molecular beam entered the electric deflector, where the molecules were dispersed according to their quantum state [19] and a pure sample of ground-state OCS was selected [20]. These molecules were aligned by a moderately intense (around 10^{11} W/cm²) laser pulse inside a velocity map imaging (VMI) spectrometer [21]. The angular confinement was probed through strong-field multiple ionization by a 30-fs laser pulse resulting in Coulomb explosion of the molecule. The produced S⁺ ions were velocity mapped onto a 40-mm-diameter position-sensitive detector consisting of a multichannel plate, a fast phosphor screen, and a high-frame-rate camera.

The alignment and ionization laser pulses were provided by an amplified femtosecond laser system at a repetition rate of 1 kHz with a center wavelength of 800 nm and a spectral bandwidth of 72 nm [22]. Directly behind the amplification stages the laser beam was split into two parts, an alignment beam and a probe beam. The alignment pulses can be compressed or stretched (negatively chirped) with an external compressor continuously to pulse durations ranging from 40 fs to 520 ps. The probe pulses were compressed to 30 fs using the standard grating-based compression setup.

*jochen.kuepper@cfel.de; <http://desy.cfel.de/cid/cmi>

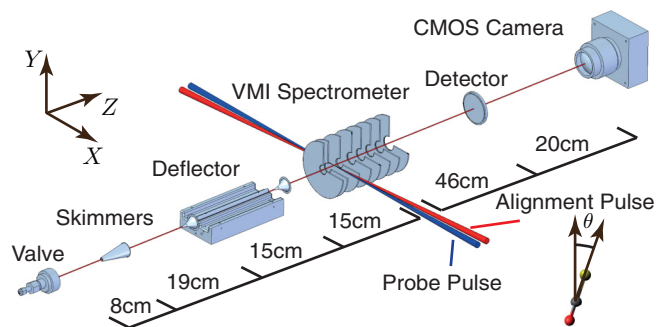


FIG. 1. (Color online) Schematic of the experimental setup, including the axis system and the definition of θ between the laboratory fixed Y axis and the molecular axis z .

Since both beams were generated by the same laser system they were inherently synchronized. Both beams were incident on a 60-cm-focal-length lens, parallel to each other, with a transverse distance of 10 mm. The foci were overlapped in space and time in the molecular beam in the center of the velocity-map-imaging spectrometer. The relative timing between the two pulses was adjusted by a motorized linear translation stage.

In our theoretical description, we solved the time-dependent Schrödinger equation [23] starting in the field-free rotational ground state and using the experimental temporal profile of the laser intensity. The angular part of the interaction potential between the molecules and the nonresonant laser field, $-I(t)\Delta\alpha\cos^2\theta/(2c\epsilon_0)$, is presented in Fig. 2(a) for $I = 6 \times 10^{11} \text{ W/cm}^2$; I is the laser intensity, $\Delta\alpha$ is the polarizability anisotropy, and θ is the angle between the alignment laser polarization, Y , and the axis of the molecule, z . Moreover, the energies of the pendular states $|\tilde{J}, M\rangle$ in that potential are depicted. Here, the $|\tilde{J}, M\rangle$ labels are used for the pendular states that correlate adiabatically with the field-free rotational states $|J, M\rangle$. To rationalize the experimental observations, we computed the degree of alignment $\langle\cos^2\theta_{2D}\rangle$ and the decomposition of the wave packet in terms of the adiabatic pendular eigenstates. Our theoretical description includes the velocity distribution of the ions after the Coulomb explosion and a volume effect model which takes into account the spatial intensity profiles of the alignment and the probe laser pulses [24].

Figure 3(a) shows the degree of alignment measured as a function of the delay between the alignment and probe laser pulses for an alignment pulse duration of 450 fs (impulsive alignment) and a peak intensity of $1.5 \times 10^{13} \text{ W/cm}^2$. These results fully agree with previous experiments and the analysis of the prominent quarter-period revival confirms that the molecules are prepared in the absolute ground state $J = 0$ [20].

Figure 3(c) shows the degree of alignment for a pulse duration of 485 ps and a peak intensity of $2.2 \times 10^{11} \text{ W/cm}^2$. The temporal laser profile is indicated by the shaded area. The rise and fall times of the pulse are 100 and 150 ps, respectively (10–90 %). The degree of alignment adiabatically follows the temporal laser profile as expected for pulses where all relevant time scales are larger than the rotational period of the molecule.

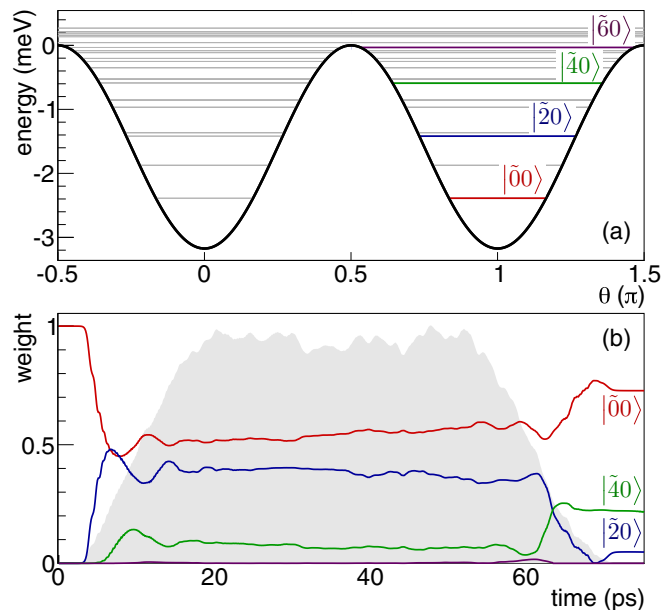


FIG. 2. (Color online) (a) Potential energy curve (black line) and energies of the pendular states in the depicted energy range (gray and colored lines) for $I = 6 \times 10^{11} \text{ W/cm}^2$. The experimentally populated adiabatic pendular states are shown in color and are labeled by $|\tilde{J}, M\rangle$. (b) The time-dependent weights of the projections of the pendular wave packet, which started from the field-free ground state, onto the pendular-state basis. The temporal laser profile is indicated by the gray area.

Figure 3(b) shows the time dependence of the degree of alignment for a pulse duration of 50 ps (FWHM in intensity) and intensities $4.5 \times 10^{10} \text{ W/cm}^2$ (blue online), $7.5 \times 10^{10} \text{ W/cm}^2$ (green online), and $6 \times 10^{11} \text{ W/cm}^2$ (red online). The 10–90 % rise time of the laser pulse is 10 ps. It is followed by a plateau where the laser intensity is approximately constant. With $\tau_{\text{rot}} \approx 82 \text{ ps}$ this places the temporal features of the pulse between adiabatic and impulsive alignment. The rising edge of the laser pulse creates a wave packet of pendular states through Raman coupling with selection rules $\Delta J = 0, \pm 2$ and $\Delta M = 0$. This wave packet propagates in the effective potential for the molecules in the laser field, giving rise to an oscillatory modulation of the degree of alignment. These oscillations are attributed to the bouncing back and forth of the wave packet in the potential. A movie depicting the wavepacket dynamics is provided in the supplementary information [25]. It resembles the librational motion of a classical pendulum.

The oscillation frequency increases with increasing peak intensity of the alignment laser, indicating the admixing of higher-angular-momentum states. Simultaneously, the amplitude of the oscillation decreases, depicting the stronger angular confinement of the molecules deeper in the potential and therefore a smaller change in the degree of alignment. The oscillations are very pronounced at the beginning of the laser pulse, but their amplitude decreases toward the end of the pulse. Initially, the phase of oscillation is defined by the rising edge; i. e., it is nearly the same for all molecules. The decrease during the laser pulse is mainly attributed to the volume effect,

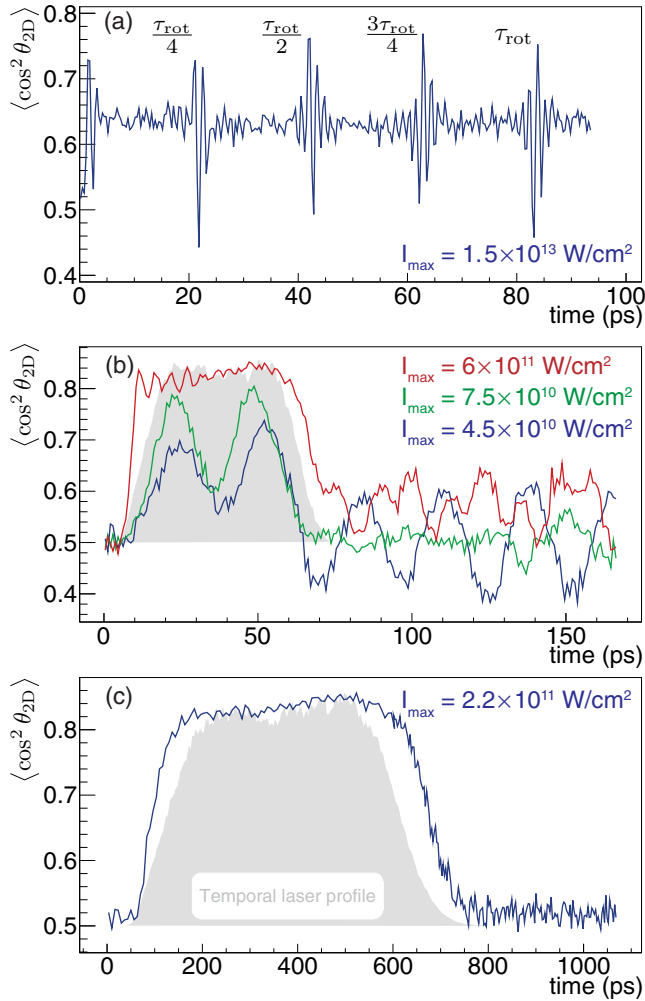


FIG. 3. (Color online) Measured degree of alignment $\langle \cos^2 \theta_{2D} \rangle$ as a function of the delay between the alignment and probe laser pulses for alignment pulse durations of (a) 450 fs, (b) 50 ps, and (c) 485 ps. The temporal profiles of the alignment laser pulses are indicated by the gray areas.

i. e., different molecules experiencing different laser intensities [24]. Additional contributions to the decrease of contrast in the amplitude of the oscillations are due to the not completely flat temporal laser-intensity profile and the anharmonic-oscillator potential, shown in Fig. 2(a).

The calculated decomposition of the wave packet in terms of its pendular-state basis for the 50-ps pulse of intensity $6 \times 10^{11} \text{ W/cm}^2$, shown in Fig. 3(b), is given in Fig. 2(b). The coefficients show rapid changes at the two edges of the pulse, whereas they keep an approximately constant value in the plateau region. Here, only $|0,0\rangle$, $|2,0\rangle$, and $|4,0\rangle$ contribute significantly to the dynamics. The oscillations in the degree of alignment are due to the temporal evolution of the phase of these pendular states. Figure 2(a) illustrates that during the pulse all contributing states are bound in the potential well. For the $4.5 \times 10^{10} \text{ W/cm}^2$ and $7.5 \times 10^{10} \text{ W/cm}^2$ pulses the pendular ground state has by far the largest contribution ($\gtrsim 0.89$) to the wave packet. Thus, the oscillations in $\langle \cos^2 \theta_{2D} \rangle$ are due to the coherence between $|0,0\rangle$ and $|2,0\rangle$, with the

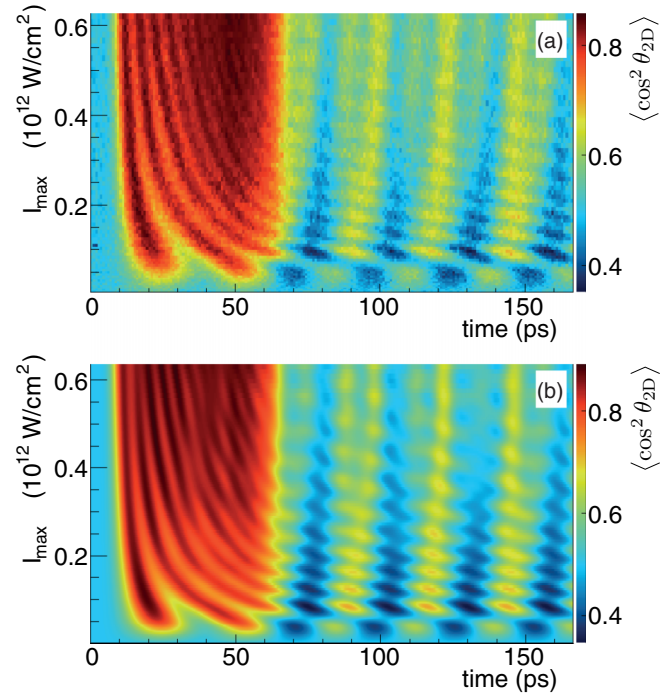


FIG. 4. (Color online) $\langle \cos^2 \theta_{2D} \rangle$ as a function of the delay between the alignment and the probe laser pulses and the peak intensity of the alignment laser pulse. The alignment pulse duration is 50 ps. (a) Experimental and (b) theoretical results.

latter being unbound for these intensities. These two-state interferences are reflected by the cosine-like oscillations of the degree of alignment.

To obtain further insight into the alignment dynamics in the intermediate regime the degree of alignment is recorded for a range of alignment pulse peak intensities as a function of time. The alignment pulse duration is 50 ps as in Fig. 3(b). A two-dimensional (2D) representation of the experimental results is shown in Fig. 4(a). The corresponding theoretical calculations are shown in Fig. 4(b). The oscillatory behavior of the degree of alignment during the laser pulse (between 10 and 50 ps) is again strongly visible. The frequencies of the oscillations are small in the low-intensity regime (*vide supra*). As the laser intensity is increased, more oscillations are observed.

Figure 4 also shows a complex behavior of the degree of alignment as soon as the laser is switched off, with a strong dependence on the intensity of the laser pulse. At low laser intensities we observed a revival structure corresponding to a single-cosine dependence due to the beating of $|0,0\rangle$ and $|2,0\rangle$. Moreover, for an intensity of $7.5 \times 10^{10} \text{ W/cm}^2$, we find that the revival structure is strongly suppressed and only a weak revival structure is observed; this is also visible in the green (gray) trace in Fig. 3(b). For these conditions, the field-free state after the laser pulse closely resembled the initial field-free state [15]. The phase between wave packet components is modified by the falling edge of the laser pulse in such a way that the revival structure is coherently switched off. This effect repeats itself for increasing laser intensities. These quantum interferences are similar to those previously observed with two appropriately delayed laser pulses [26], but now it is achieved

with a single pulse of appropriate duration and intensity. The computational results in Fig. 4(b) are in excellent agreement with the experimental results in Fig. 4(a). For $I_{\max} \approx 6 \times 10^{10}$ W/cm² these computations predict no alignment once the pulse is off with small oscillations around the mean value of $\langle \cos^2\theta_{2D} \rangle \approx 0.50$. The incomplete suppression of the experimental alignment structure is attributed to the volume effect and, thus, the simultaneous observation of dynamics for different field strengths.

In conclusion, we studied the time-dependent alignment behavior of state-selected OCS molecules in their absolute ground state for a pulse duration in the intermediate regime, between impulsive and adiabatic alignment. We observed strong oscillations in the degree of alignment during the laser pulse. These oscillations are attributed to the propagation of a wave packet in the potential of the molecule in the alignment laser field. The observed motion is the quantum analog of an oscillating pendulum. Our results show the opportunity to initiate and stop wave packet motion within a short period and by a single laser pulse. It provides an effective coherent control scheme of molecular motion.

The wave packet dynamics inside the effective potential has implications on the performance of experiments with laser-aligned molecules such as the investigation of molecular-frame photoelectron angular distributions [9], the detection of structural changes via x-ray and electron diffraction [6,11,27,28], and photoelectron holography from within [10], because typically a strong degree of alignment is required for these experiments. Reducing the jitter of the relative timing and applying the appropriate delay of the alignment and probe laser allows for the strongest degree of alignment to be achieved,

since the molecules can be probed at one of the maxima of $\langle \cos^2\theta \rangle$ of the pendular state dynamics. This holds especially for large molecules with rotational periods on the order of a few nanoseconds (ns), where nonadiabatic effects will start to play a role even with ns laser pulses that are often employed to strongly fix molecules in space.

The observed pendular motion has implications on the performance of ultrafast molecular switches based on internal-rotation dynamics [29,30]. The torsional motion of non-rigid quantum objects [7,31] or surface adsorbed molecules [29,32,33] is governed by a 2π -periodic potential about the torsional or dihedral angle [34]. Variations in the relative alignment of the two moieties will lead to variations in, e. g., the current through a molecular switch [31,35]. Inducing a wave packet of the internal rotation to coherently switch the system and terminating the motion in the desired position by the end of the laser pulse [36–38] would work even when the surrounding media is not dissipative.

This work has been supported by the excellence cluster “The Hamburg Center for Ultrafast Imaging—Structure, Dynamics, and Control of Matter at the Atomic Scale” of the Deutsche Forschungsgemeinschaft, including the Mildred Dresselhaus Award for R.G.F. R.G.F. also gratefully acknowledges financial support by the Spanish Ministry of Science FIS2011-24540 (MICINN), the Grants No. P11-FQM-7276 and No. FQM-4643 (Junta de Andalucía), and the Andalusian research group FQM-207. J.J.O. acknowledges support through the research plan of the Universidad de Granada. N.L.M.M. gratefully acknowledges support from a fellowship of the Joachim Herz Stiftung.

-
- [1] H. J. Loesch and A. Remscheid, *J. Chem. Phys.* **93**, 4779 (1990).
- [2] B. Friedrich and D. R. Herschbach, *Nature* **353**, 412 (1991).
- [3] B. Friedrich and D. Herschbach, *Phys. Rev. Lett.* **74**, 4623 (1995).
- [4] H. Stapelfeldt and T. Seideman, *Rev. Mod. Phys.* **75**, 543 (2003).
- [5] K. Nauta and R. E. Miller, *Science* **283**, 1895 (1999).
- [6] J. C. H. Spence and R. B. Doak, *Phys. Rev. Lett.* **92**, 198102 (2004).
- [7] C. B. Madsen, L. B. Madsen, S. S. Viftrup, M. P. Johansson, T. B. Poulsen, L. Holmegaard, V. Kumarappan, K. A. Jørgensen, and H. Stapelfeldt, *Phys. Rev. Lett.* **102**, 073007 (2009).
- [8] S. M. Purcell and P. F. Barker, *Phys. Rev. Lett.* **103**, 153001 (2009).
- [9] L. Holmegaard, J. L. Hansen, L. Kalhøj, S. L. Kragh, H. Stapelfeldt, F. Filsinger, J. Küpper, G. Meijer, D. Dimitrovski, M. Abu-samha *et al.*, *Nat. Phys.* **6**, 428 (2010).
- [10] R. Boll, D. Anielski, C. Bostedt, J. D. Bozek, L. Christensen, R. Coffee, S. De, P. Decleva, S. W. Epp, B. Erk *et al.*, *Phys. Rev. A* **88**, 061402 (2013).
- [11] J. Küpper, S. Stern, L. Holmegaard, F. Filsinger, A. Rouzée, A. Rudenko, P. Johansson, A. V. Martin, M. Adolph, A. Aquila *et al.*, *Phys. Rev. Lett.* **112**, 083002 (2014).
- [12] P. A. Block, E. J. Bohac, and R. E. Miller, *Phys. Rev. Lett.* **68**, 1303 (1992).
- [13] W. Kim and P. M. Felker, *J. Chem. Phys.* **104**, 1147 (1996).
- [14] H. Stapelfeldt, E. Constant, and P. B. Corkum, *Phys. Rev. Lett.* **74**, 3780 (1995).
- [15] J. Ortigoso, M. Rodriguez, M. Gupta, and B. Friedrich, *J. Chem. Phys.* **110**, 3870 (1999).
- [16] T. Seideman, *Phys. Rev. Lett.* **83**, 4971 (1999).
- [17] R. Torres, R. de Nalda, and J. P. Marangos, *Phys. Rev. A* **72**, 023420 (2005).
- [18] D. Irimia, D. Dobrikov, R. Kortekaas, H. Voet, D. A. van den Ende, W. A. Groen, and M. H. M. Janssen, *Rev. Sci. Instrum.* **80**, 113303 (2009).
- [19] F. Filsinger, J. Küpper, G. Meijer, L. Holmegaard, J. H. Nielsen, I. Nevo, J. L. Hansen, and H. Stapelfeldt, *J. Chem. Phys.* **131**, 064309 (2009).
- [20] J. H. Nielsen, P. Simesen, C. Z. Bisgaard, H. Stapelfeldt, F. Filsinger, B. Friedrich, G. Meijer, and J. Küpper, *Phys. Chem. Chem. Phys.* **13**, 18971 (2011).
- [21] A. T. J. B. Eppink and D. H. Parker, *Rev. Sci. Instrum.* **68**, 3477 (1997).
- [22] S. Trippel, T. Mullins, N. L. M. Müller, J. S. Kienitz, K. Długołęcki, and J. Küpper, *Mol. Phys.* **111**, 1738 (2013).
- [23] P. Sanchez-Moreno, R. González-Férez, and P. Schmelcher, *Phys. Rev. A* **76**, 053413 (2007).
- [24] J. J. Omiste, M. Gaertner, P. Schmelcher, R. González-Férez, L. Holmegaard, J. H. Nielsen, H. Stapelfeldt, and J. Küpper, *Phys. Chem. Chem. Phys.* **13**, 18815 (2011).

- [25] See Supplemental Material at <http://link.aps.org/supplemental/10.1103/PhysRevA.89.051401> for a movie that shows the evolution of the probability density of the wave packet of the pendular states of OCS during the 50-ps-long laser pulse.
- [26] K. F. Lee, D. M. Villeneuve, P. B. Corkum, and E. A. Shapiro, *Phys. Rev. Lett.* **93**, 233601 (2004).
- [27] F. Filsinger, G. Meijer, H. Stapelfeldt, H. Chapman, and J. Küpper, *Phys. Chem. Chem. Phys.* **13**, 2076 (2011).
- [28] C. J. Hensley, J. Yang, and M. Centurion, *Phys. Rev. Lett.* **109**, 133202 (2012).
- [29] B. Y. Choi, S. J. Kahng, S. Kim, H. Kim, H. W. Kim, Y. J. Song, J. Ihm, and Y. Kuk, *Phys. Rev. Lett.* **96**, 156106 (2006).
- [30] T. Avellini, H. Li, A. Coskun, G. Barin, A. Trabolsi, A. N. Basuray, S. K. Dey, A. Credi, S. Silvi, J. F. Stoddart, and M. Venturi, *Angew. Chem. Int. Ed.* **51**, 1611 (2012).
- [31] S. Ramakrishna and T. Seideman, *Phys. Rev. Lett.* **99**, 103001 (2007).
- [32] Z. J. Donhauser, B. A. Mantooth, K. F. Kelly, L. A. Bumm, J. D. Monnell, J. J. Stapleton, D. W. Price, A. M. Rawlett, D. L. Allara, J. M. Tour, and P. S. Weiss, *Science* **292**, 2303 (2001).
- [33] M. G. Reuter, M. Sukharev, and T. Seideman, *Phys. Rev. Lett.* **101**, 208303 (2008).
- [34] W. Gordy and R. L. Cook, *Microwave Molecular Spectra*, 3rd ed. (John Wiley & Sons, New York, 1984).
- [35] M. del Valle, R. Gutiérrez, C. Tejedor, and G. Cuniberti, *Nat. Nanotechnol.* **2**, 176 (2007).
- [36] F. Großmann, L. Feng, G. Schmidt, T. Kunert, and R. Schmidt, *Europhys. Lett.* **60**, 201 (2002).
- [37] M. Barbatti, S. Belz, M. Leibscher, H. Lischka, and J. Manz, *Chem. Phys.* **350**, 145 (2008).
- [38] S. M. Parker, M. A. Ratner, and T. Seideman, *J. Chem. Phys.* **135**, 224301 (2011).